Geophysica (1996), 32(1-2), 109-125

Simulation of Stationary Waves and Their Interannual Variations With an Adequately Resolved Linear p-coordinate Model

Kimmo Ruosteenoja and Carl Fortelius

Department of Meteorology, P.O.Box 4, 00014 University of Helsinki, Finland

(Received: December 1995; Accepted: July 1996)

Abstract

Stationary waves were simulated with a linear semi-spectral model, using an equidistant grid with a spacing of 1.8° in the meridional direction and 16 non-equidistant model levels between 30 hPa and 1000 hPa. A systematic study showed that this resolution produces simulations in which the discretization errors are negligibly small.

The model simulates wintertime climatological stationary waves in the northern extratropics well, the correlation with the observed patterns varying from 0.95 at the surface to ~ 0.8 in the upper troposphere and lower stratosphere. The quality of the simulation is comparable to that obtained with previous σ coordinate models.

In studying the interannual variability of stationary waves, the correlations between the simulated and observed anomalies are lower but still moderately high, ~ 0.4-0.6. The simulated anomalies in the stationary waves are mainly excited by the fluxes of heat and momentum in transient eddies, although nonlinear momentum fluxes in the stationary waves themselves are important as well. The direct response to anomalous diabatic heating, by contrast, proved to be fairly insignificant.

Key words: stationary waves, climate anomalies, linear climate model, numerical resolution

1. Introduction

The climate in a certain area, e.g. in Northern Europe, is determined both by the atmospheric zonally-averaged time mean flow and by deviations in the east-west direction. These deviations, called stationary waves, are primarily forced by diabatic heating and the vertical velocities at the lower boundary due to zonally-varying orography. In addition, the distribution of the stationary waves is modified by nonlinear fluxes of heat and momentum in transient eddies. The stationary wave pattern of a given season varies from year to year, and these fluctuations account for the majority of interannual variability in weather conditions in the middle latitudes. In the longer term, global climate changes, e.g. those related to an increase in the concentration of greenhouse gases, are likely to be accompanied by changes in the stationary wave pattern. Such changes may significantly affect local climate conditions. Thus compelling reasons exist for studying the mechanisms behind stationary waves and their fluctuations.

The distribution of stationary waves is simulated most reliably by atmospheric general circulation models, but such simulations do not explain the importance of the various factors in forcing stationary waves. Formally, the contribution of each forcing function can be found by simulating the waves with equations linearized about the temporally-averaged zonal mean state. When a model based on such linearized equations is used as a diagnostic tool in analyzing the stationary waves, the nonlinear fluxes of heat and momentum in the stationary waves themselves can be treated as external forcing functions, as well as the forcing by diabatic heating, mountains and transient eddies. All these forcing functions can be derived from observations or from the output of a general circulation model.

A linear model works well in the middle latitudes, i.e. in areas where the zonal mean zonal velocity $[u]$ is far from zero. Stationary waves are mainly excited by midlatitude forcing. Close to the so-called critical latitudes in low latitudes $[u]$ vanishes, and inviscid linear simulation fails (*Held*, 1983). Using nonzero damping in the equation of momentum and adequate numerical resolution in the meridional direction, the singularity at the critical latitudes can be eliminated (*Nigam*, 1985; *Ruosteenoja*, 1988), as a result of which the inadequate description of stationary waves in the tropics does not seriously affect the simulation in middle and high latitudes.

Climatological stationary waves as a linear response to forcing functions derived from atmospheric observations have been calculated in several studies. In low-resolution simulations, the quality of simulation has been modest. For example, *Ruosteenoja* (1991) found at best a correlation of 0.54 between the observed stationary waves and those simulated with a linear two-layer model. Other papers do not generally report correlations or other quantitative measures for the similarity of the observed and simulated patterns. Still, a subjective inspection shows that the quality in high-resolution studies (e.g., *Valdes* and *Hoskins*, 1989, hereafter VH) is much better. An important factor that makes the simulation of the observed stationary waves difficult is uncertainty in the forcing functions. Diabatic heating is poorly known, for instance.

Another possibility is to derive the forcing functions from the output of a general circulation model. This forcing is then free from observational errors, and both the GCM and the linear model can use the same resolution, so that the numerical errors in both models are comparable. This approach has yielded successful linear simulations (e.g., *Nigam et al.*, 1988). The success of linear models in simulating the GCM responses proves the applicability of linear modelling, provided that numerical resolution is adequate and the forcing functions are known sufficiently well. Using a linear model for interpreting GCM results would be the most natural way to study the genesis of stationary waves in the greenhouse climate.

One purpose of the present study is to investigate how interannual variations in forcing functions account for anomalies in the stationary waves. Before doing that, we seek the number of levels in the vertical and grid points in the horizontal direction that assures adequate numerical resolution in the model. *Lindzen* and *Fox-Rabinovitz* (1989) discussed this problem using scale analysis, but their later experimental paper (*Fox-Rabinovitz* and *Lindzen*, 1993) did not present any numerical experiments that would

confirm their theoretical analysis for linear models. Here we study the effect of numerical resolution by systematically varying the resolution in both directions.

As another test, we calculate the climatological mean stationary waves as a linear response to forcing functions inferred from observations. The correctness of the climatological mean simulation is a necessary but not a sufficient condition for the fitness of the model for studying seasonal anomalies. The quality of the climatological response given by our isobaric coordinate model is compared with that obtained with a σ coordinate model by VH.

The observational data base for this study consists of circulation statistics for the ten winter seasons (December-February) from 1979/80 to 1988/89, compiled by *Hoskins et al.* (1989) from the analyses of the European Centre for Medium Range Weather Forecasts. The analyzed quantities are given on 12 pressure levels ranging from 1000 hPa to 30 hPa; the horizontal resolution is 5° in latitude and longitude.

2. *Model description*

Stationary waves are diagnosed by a linear primitive equation model with pressure (p) as the vertical coordinate; a detailed description of the model is presented in Ruosteenoja (1993). For example, the thermodynamic equation as linearized about the zonal mean state takes the form:

$$\frac{[u]}{a\cos\phi}\frac{\partial T^*}{\partial\lambda}+\frac{v^*}{a}\frac{\partial[T]}{\partial\phi}-S_p\omega^*-F_T=Q+T_h+S_h \tag{1}$$

where a is the radius of the Earth, and λ and ϕ the longitude and latitude. (u, v) is the zonal and ω the p-coordinate vertical velocity, and T the temperature. [ ] denotes a zonal mean and ( )* a deviation from that. The mean meridional circulation is not included in the equations. S_p is the zonal mean of static stability and F_T a damping term (see below). The rhs of Eq. (1) contains the forcing terms: Q stands for diabatic heating, and T_h and S_h are the nonlinear terms associated with 3-dimensional heat fluxes by transient and stationary eddies, respectively. Analogous forcing terms due to momentum flux convergence appear on the rhs of the zonal and meridional momentum equation. In addition, the model contains the continuity and hydrostatic equations. Forcing due to vertical motions associated with the orography is given as a lower boundary condition in the continuity equation.

In the zonal direction, each model variable ( )* is expanded in a Fourier series. The truncation point is 8; larger wavenumbers give an insignificant contribution to the amplitude of stationary waves. In the meridional and vertical direction, the model uses finite differences on a staggered grid.

In the meridional direction, grid points are located uniformly. In the vertical, the levels are determined by an iterative algorithm. In the troposphere and lower stratosphere between ~ 150 and ~ 870 hPa, the levels are located uniformly in p, in the stratosphere, between ~ 150 hPa and the model top (30 hPa), uniformly in ln p. The p

coordinate distance between the two uppermost levels is 0.2 times the level spacing in the troposphere. Near the lower boundary, the distance between the levels decreases again. An example of the placement of model levels is shown in Fig. 1.

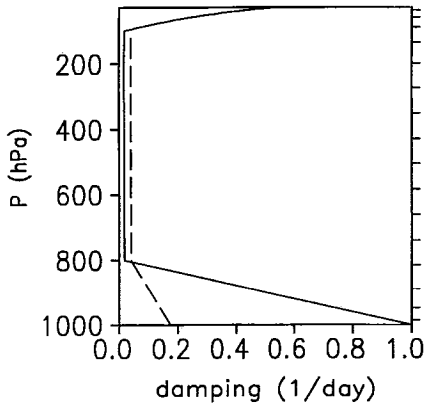

Fig. 1. Vertical distribution of the coefficients of Rayleigh friction K_m (solid line) and Newtonian cooling K_T (dashed line). Above the 100 hPa level the two lines coincide. The tick marks to the right indicate the placement of the 16 model levels used in Section 4.

The damping terms in the equations include a linear Rayleigh friction/Newtonian cooling and a ∇^4-type horizontal diffusion. The diffusion coefficient is constant (10^{15} $m^4 s^{-1}$) in both the momentum and the thermodynamic equations. In contrast, the friction (K_m) and Newtonian cooling (K_T) coefficients vary as a function of p. As shown in Fig. 1, enhanced damping is applied both in the boundary layer and in the stratosphere. The numerical values of the Newtonian cooling coefficients in the troposphere are close to those applied by VH. The purpose of the logarithmically increasing damping in the stratospheric sponge layer is to eliminate artificial wave reflections from the top. We use a stronger stratospheric damping than VH, since our model top is located as low as 30 hPa; enhanced stratospheric damping is applied in the momentum equations as well. In addition, we use weak mechanical damping everywhere in the troposphere. In the boundary layer, our friction coefficients are somewhat weaker than in VH. Below the stratospheric sponge layer the model response proved to be rather insensitive to the exact values of the damping coefficient.

The zonal mean state used in the linear model is defined by the average zonal wind and static stability over the ten winters (Fig. 2). The meridional temperature gradient $\frac{\partial[T]}{\partial\phi}$ appearing in (1) is expressed in terms of $[u]$ applying the thermal wind law. In the interpolation into the model grid, 2-dimensional spline functions were used.

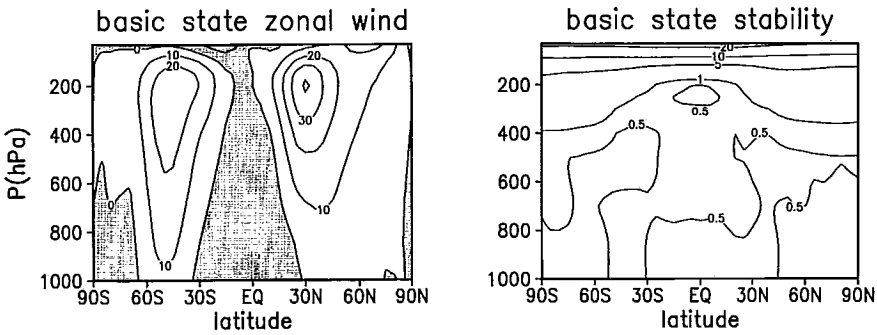

Fig. 2. Basic state zonal wind [u] and static stability S_p used in the experiments. The zonal wind is analysed with a contour interval of 10 ms^{-1}, while the stability contours are drawn at 0.5, 1, 5, 10, and 20 $K(kPa)^{-1}$.

3. *The effect of vertical and meridional resolution*

The need for numerical resolution in a linear model depends on the structure of the basic state and the distribution of the damping parameters. The required number of levels in the vertical and grid points in the meridional direction are found by running the model with an extremely high resolution and comparing this control simulation with solutions obtained at several coarser resolutions. Unfortunately, the computing capacity available did not allow running the model with a resolution simultaneously very high in both directions. We therefore study the need for vertical and meridional resolution separately.

In the meridional and vertical directions, where the model equations are solved on a finite grid, the fine-scale structures generated by the critical latitudes can affect the large-scale solution. In the zonal direction, by contrast, each harmonic component is calculated separately, and different scales are totally independent. In the present model there is therefore no need for particularly high resolution in the zonal direction.

As a measure of the quality of the numerical solution, we use the normalized rms difference

$$D_{NORM} = \sqrt{\frac{\overline{\left(z_L^* - z_H^*\right)^2}}{\overline{z_H^{*2}}}} \tag{2}$$

where z^* denotes the stationary eddy geopotential height and the indices L and H refer to the numerical solutions obtained at low and high resolutions. $\overline{(\ )}$ denotes a global mean over an isobaric level. The quality of the simulation is studied separately for each zonal wavenumber m.

For investigating very small differences, D_{NORM} is a more convenient quantity than the correlation coefficient, which would be very close to unity. In the next section, we

study the agreement between the observed and linearly simulated fields. In that case the differences are much larger than the numerical errors studied here, and consequently correlation is a more illustrative quantity.

Geopotential height is chosen as the variable to be studied because we are mainly interested in the simulation in extratropical regions. Through the geostrophic and hydrostatic relations, smallness of the numerical error in z^* implies a good simulation of other model variables (u^*, v^*, T^*).

The numerical resolution is considered "adequate" when $D_{NORM} \leq 0.1$. One can show that this value of D_{NORM} implies that the correlation between the patterns is certainly greater than 0.995. Later in this paper forcing functions will be derived from observations. Inaccuracies in the forcing, etc., then appear to cause errors much larger than 10 %, and consequently numerical errors are unimportant if the above condition is fulfilled.

In studying the numerical errors caused by the discretization of the model, we prefer a simple analytically-determined forcing to that inferred from observations. When the model is run at a low resolution, details in observation-based forcing functions would remain unresolved, and such errors could not be separated from those caused by the low numerical resolution in the model equations. The discrete model equations can be written in the form of a matrix equation, the coefficient matrix being independent of the forcing, and evidently the resolution requirements are approximately the same regardless of which kind of forcing is used. In the experiments to be discussed in this section, we use a local thermal forcing that is analogous to that used by *Hoskins* and *Karoly* (1981). The horizontal distribution of the heating is:

$$Q(\lambda,\phi,p)=Q_0(p)\cos\left(\frac{\pi R^2}{2}\right)$$

if $R \leq 1$ and zero elsewhere, with

$$R^2=\left(\frac{\phi-\phi_0}{8^\circ}\right)^2+\left(\frac{\lambda-\lambda_0}{32^\circ}\right)^2$$

The centre of the forcing is located at ϕ_0 = 15°N. This relatively low latitude was chosen since the scale analysis of *Lindzen* and *Fox-Rabinovitz* (1989) shows that the need for vertical resolution is highest in low latitudes. Moreover, the response to a low-latitude forcing is evidently most sensitive to meridional resolution, because of the vicinity of the critical latitude.

The vertical distribution of the heating is sinusoidal with a maximum of Q_0 = 2.5 K/day at 600 hPa and zero points at 200 hPa and 1000 hPa. Above the 200 hPa level, Q is set equal to zero.

The effect of vertical resolution was studied by letting the number of levels L vary between 2 and 30. These numerical solutions were compared with that obtained

with the resolution of L = 60; this resolution is evidently high enough to give a simulation virtually free from errors due to vertical discretization. The normalized rms differences between the low and high resolution responses are given in Fig. 3. The numerical solution converges very rapidly as a function of L. A vertical resolution as low as L = 10 appears to give a numerical error of ~ 10%. For an error of ~ 1%, 25-30 levels are required.

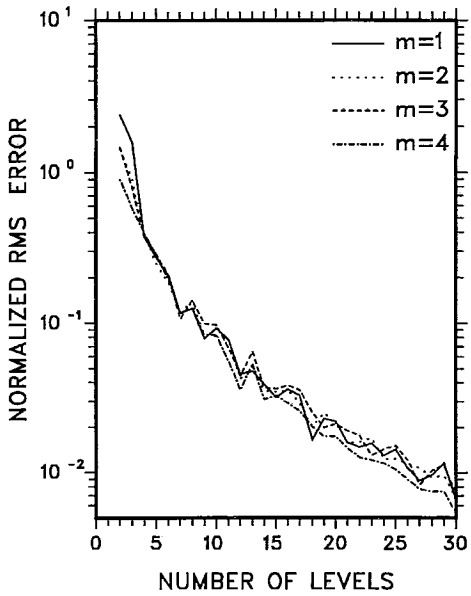

Fig. 3. The normalized rms error D_{NORM} of z^* (300 hPa) as a function of the number of levels for wavenumbers m=1-4. The control solution is obtained with 60 levels. The number of grid points in the meridional direction between the poles is N=100 in all experiments.

If the forcing were located in the middle or high latitudes, a still coarser vertical resolution might be adequate (*Lindzen* and *Fox-Rabinovitz*, 1989). Responses to equatorial forcings are evidently more sensitive. In the next section, there is also some forcing near the equator. In the present model with a moderately large horizontal diffusion, however, stationary waves induced by equatorial forcing are effectively absorbed at critical latitudes. Elsewhere stationary waves are almost exclusively extratropically forced, and are accordingly correctly simulated with about 10 levels.

In studying the sensitivity to meridional resolution, the number of grid points between the poles was varied, while the number of levels was kept equal to 16; the error due to vertical discretization is then negligible (~ 3%). The control simulation was calculated with N=400 grid points, and the numerical errors of the simulations with N=100, 200 and 300 are given in Table 1. When N=100, the numerical error for wavenumber m=1 is ~ 10%, and < 10% for larger wavenumbers. For N=200 and 300, numerical errors are substantially smaller.

Table 1. Normalized rms error of the numerical solution calculated with 100, 200 and 300 grid points between the poles for zonal wavenumbers m=1-4. The control solution was obtained with 400 grid points. The number of levels is L=16 in all experiments.

	N = 100	N = 200	N =300
m=1	0.1010	0.0287	0.0102
m=2	0.0805	0.0153	0.0039
m=3	0.0638	0.0112	0.0026
m=4	0.0403	0.0072	0.0015

Ruosteenoja (1988) showed that, in the case of an inadequately-resolved critical latitude, the amplitude of the response tends to oscillate as a function of N. In order to investigate this possibility, we ran the model with consecutive values of N ranging from N=92 to 100. The numerical errors associated with m=1 decreased almost monotonically from 0.1144 to 0.1010 when N increased from 92 to 100, with fluctuations of only ~ 1%-units around the monotonic trend. Larger wavenumber components behaved analogously.

The high-resolution simulations (L=60, N=100) and (L=16, N=400) require so much computer memory capacity that they had to be run with a slow virtual memory computer. We therefore had to limit the detailed numerical study to zonal wavenumbers m=1-4. These wavenumbers account for the bulk of the model response. More importantly, our results indicate that the convergence as a function of N is more rapid for high than low wavenumber components, whereas all components converge almost equally rapidly as a function of L. It is therefore evident that wavenumbers m=5-8 do not introduce significant numerical error into the total response if $L \geq 10$ and $N \geq 100$.

The requirements for horizontal and vertical resolution deduced in this study cannot be directly generalized to other linear models. In the absence of horizontal diffusion, for example, a much denser meridional grid is required (*Ruosteenoja*, 1988). Similarly, the need for vertical resolution might be sensitive to damping parameters. We made an experiment in which the convergence as a function of L was studied without applying enhanced damping in the stratosphere, but the rate of convergence remained almost unchanged. In our simulations the sponge layer is evidently so weak and thin that it does not significantly affect the numerical accuracy. The sensitivity to a more intense sponge layer may be greater.

In many models the top is located higher than 30 hPa; the number of the levels must then be increased accordingly. In addition, the sensitivity to the resolution may depend on the structure of the basic state. In the future, we plan to study the dependence of the convergence of the numerical solution on model parameters more thoroughly.

In the experiments to be discussed hereafter, we use 100 grid points between the poles, i.e., a meridional resolution of 1.8°. In the vertical, we use 16 levels instead of the ~ 10 that would be enough to make the numerical error negligibly small. The largest interval between two adjacent pressure levels is then 77 hPa. This resolution

was chosen in order to avoid interpolation of the forcing functions onto a vertical grid substantially coarser than the original one. Such an interpolation would smooth essential features of the forcing functions.

4. *Analysis of the observed waves*

The present investigation concentrates on the stationary waves of the winter-time (December - February) middle latitude flow of the northern hemisphere. Here interannual variability is mainly associated with stationary eddies, which contribute about 75% of the interannual variance of the geopotential height field. Only about 25% is associated with zonally symmetric variability.

The principal diagnostic tool used for assessing the relative importance of the various forcings is the correlation between the observed and simulated waves. Although the responses to individual forcings are additive, this is not true for a non-linear measure such as the correlation coefficient. The importance of a particular forcing is judged therefore by the decrease of correlation that occurs when the contribution of that particular forcing is left out of the total response.

Climatological conditions are defined by taking the average over the ten winters covered by the data base, and anomalies are defined as the difference between conditions during a given winter season and the climatology. In principle, anomalies in the simulated waves may be caused either by anomalous forcing or by anomalous wave propagation, associated with fluctuations in the zonally symmetric state. The response may be sensitive to details in the zonal mean state, and the latter mechanism is thus potentially important. However, the climatological basic state was used throughout, because letting the basic state vary from year to year was not found to improve the correspondence between simulated and observed anomalies. Given the rather coarse resolution of the data base, the anomalies in the basic state may not be described with sufficient accuracy. The climatological zonal mean state is smoother than that of an individual year, and hence more accurately determined by the observations.

For comparison with the observed waves the model results were interpolated linearly to 12 standard pressure levels. The observations have been smoothed by spectral truncation at two-dimensional wave number 12 in order to remove features that the model cannot be expected to reproduce.

4.1 *Empirical forcing*

The forcing due to diabatic heating and mountain ranges, as well as the fluxes of momentum and heat in transient and stationary eddies are computed for each winter. Forcing due to fluxes of momentum and heat is computed from the circulation statistics using standard numerical techniques; for the exact expressions, see *Ruosteenoja* (1993). The diabatic heating is determined as a residual term in the thermodynamic energy equation as described in *Fortelius* and *Holopainen* (1990). Although the tropical

heating is somewhat uncertain, this technique should yield adequate estimates of the heating in middle latitudes, which is much more important for the middle latitude response.

In contrast with the other empirical forcing functions, the mountain forcing cannot be unambiguously represented in the linear p-coordinate model. Mountains influence the atmospheric flow by forcing vertical motion at the surface, and in isobaric coordinates this forcing appears as a boundary condition for ω: $\omega_s = \frac{\partial p}{\partial t} + V_s \cdot \nabla p_s$, where the subindex s refers to a value at the surface. In the linear model the boundary condition is applied at the lowest half level (1000 hPa) which does not coincide with the true surface. Moreover, neither V_s nor p_s are included in the isobaric analyses used. In the present study the mountain forcing is therefore estimated simply as the zonally asymmetric part of the expression $-g\rho_0 V_{85} \cdot \nabla h$, where V_{85} is the observed time-mean wind at 850 hPa, a constant value of 1.077 kg m^{-3} is used for ρ_0 and h is the orographic height. This mountain forcing includes the interaction of the stationary waves with orography, and was found to give a better simulation of the climatological stationary waves than did a formulation involving only the zonal mean wind $[u]$. However, the solution was further improved by suppressing all orographic forcing north of 60 °*N*. Apparently this is related to a very intense pattern of vertical motion around Greenland, in a region where the weakness of the basic state zonal wind (Fig. 2) makes the solution sensitive to small perturbations both in the forcing and in the basic state.

Small-scale noise in the empirically-determined forcing was removed by expansion to spherical harmonics followed by triangular truncation at two-dimensional wave number 12. No forcing is applied in the stratospheric sponge layer above 100 hPa.

4.2 The climatological waves

Figure 4 shows the observed and simulated climatological stationary eddy geopotential height at 250 and at 1000 hPa. In the lower troposphere the simulated eddies match the observed ones very closely. Near the tropopause the correspondence is slightly less close, possibly because the wave amplitude is larger there, so that nonlinearity is more important. In middle latitudes the simulated and observed waves are well in phase throughout the troposphere, but in the upper troposphere the simulated waves tend to be too weak.

To the north of 60°*N*, the simulated waves at 250 hPa are excessively strong and out of phase with the observed eddies. The failure of the linear model here is evidently at least partly related to the weak basic state zonal wind, which even changes sign in these latitudes. The weak basic state flow increases the relative importance of the approximately represented non-linear terms, and the presence of a polar critical latitude makes the response sensitive to the formulation of the damping terms (e.g. VH, *Ruosteenoja*, 1988).

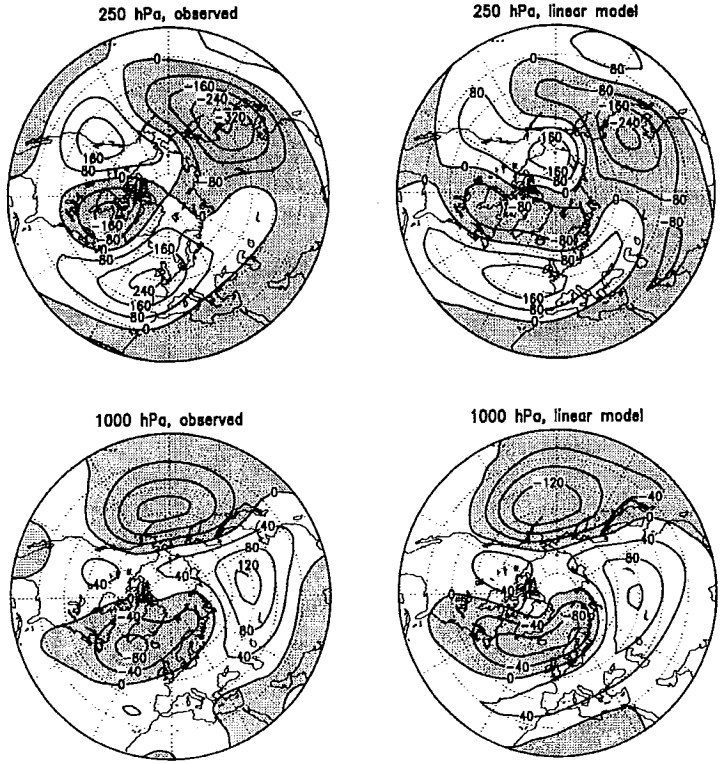

Fig. 4. Observed and simulated climatological stationary eddy height fields at 250 and 1000 hPa. The contour interval is 80 m at the upper level and 40 m at the lower level; shading indicates negative values.

In middle and high latitudes, the simulated wave patterns resemble rather closely the climatological stream function patterns obtained by VH (their Fig. 22) using a linear σ coordinate model. The similarity includes salient errors such as the spurious upper trough over the Greenland Sea, and a corresponding excessively strong ridge near the date line.

Figure 5 shows the correlation between the observed and simulated waves as a function of pressure for various forcing combinations. When all the forcings are included, the degree of correlation is around 0.8 in the upper and middle troposphere, increasing to 0.95 at 1000 hPa (the value of D_{NORM} is 0.37 at 1000 hPa). Omitting any one of the forcing functions is seen to degrade the simulation considerably. Using this measure, feedback from the stationary eddies themselves is the most important single forcing. In the lower troposphere orography and transient eddies are equally important. The midlatitude response to diabatic heating has a baroclinic structure with a node near 800 hPa. Accordingly, the diabatic heating has its largest influence on the correlation in the upper troposphere and at the surface.

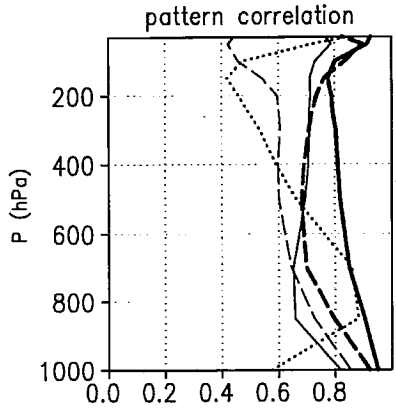

Fig. 5. Vertical distribution of the pattern correlation to the north of latitude 30°N between the climatological stationary wave fields as observed and as computed for various combinations of the forcing due to orography (O), diabatic heating (D), transient eddies (T), and stationary eddies (S). Heavy solid line: O+D+T+S, heavy dashed line: D+T+S, dotted line: O+T+S, light solid line: O+D+S, light dashed line: O+D+T.

Stationary and transient eddies contribute to the eddy forcing both by their momentum fluxes and by their heat fluxes. In the forcing by transients, both components are of similar importance, whereas in the forcing by stationary eddies the momentum fluxes dominate (not shown).

4.3 Interannual variability

Relative to the climatological amplitude of the stationary waves, their interannual variability is largest at 850 hPa. Figure 6a shows the interannual standard deviation of the observed eddies at this level. Maxima are found over the northern Pacific Ocean and the North Atlantic. The simulated variability (Fig. 6b), obtained by letting the forcing vary from year to year, exhibits both realistic and unrealistic features. The overall shape of the distributions is similar: the two oceanic maxima are reproduced with the correct relative intensity and an Asian maximum is present in both panels. On the other hand, the model severely overestimates the variability over the Eurasian continent and in general to the north of latitude 60°N. (In the latter region the model also failed to reproduce the climatological waves.)

Figure 7 shows the interannual standard deviation of the 850 hPa linear responses to the different forcings. Fluctuations in the orographic forcing (panel a) produce variability mainly in the vicinity of the Tibetan plateau, while anomalous diabatic heating (panel b) is of minor importance everywhere. Most of the simulated variability is clearly due to anomalous forcing by transient (panel c) and stationary (panel d) eddies. Although the individual contributions to the standard deviation are not strictly additive, fluctuations in the forcing by transient eddies appear to be about equally important in the Pacific and the Atlantic, while anomalous forcing by stationary eddies

gives rise to interannual variability mainly over the Pacific Ocean and over the Eurasian continent. Both kinds of eddy forcing seem to be jointly responsible for the unrealistic variability in high latitudes.

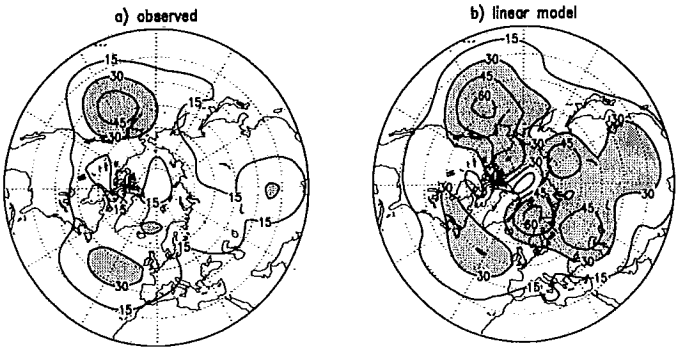

Fig. 6. Standard deviation of the interannual variability of the zonally asymmetric wintertime height field at 850 hPa (a) as observed and (b) as reproduced by the linear model using the total forcing. The contour interval is 15 m and values in excess of 30 m are indicated by shading.

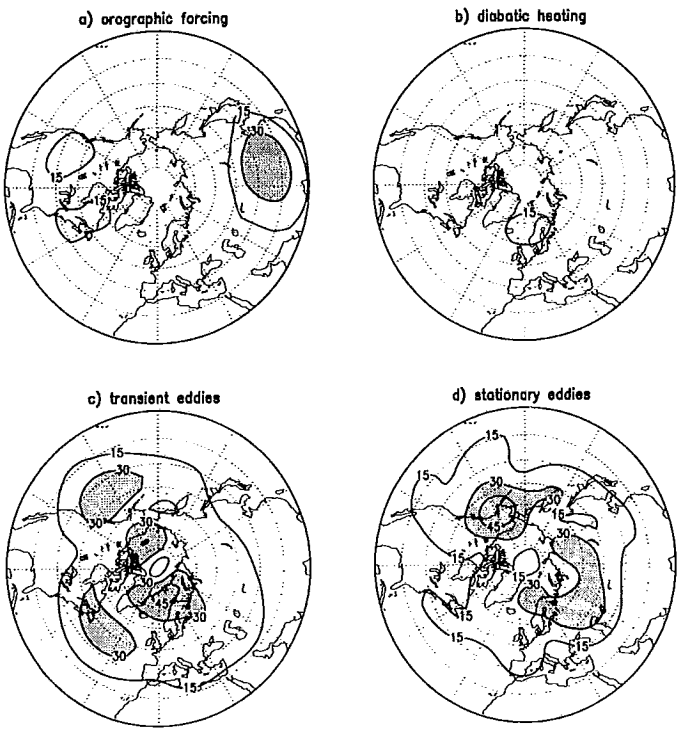

Fig. 7. Standard deviation of the interannual variability of the zonally asymmetric height field at 850 hPa computed separately for the forcing due to orography (a), diabatic heating (b), transient eddies (c) and stationary eddies (d). The contour interval is 15 m and values in excess of 30 m are indicated by shading.

Figure 8 shows vertical profiles of the correlation between the observed and simulated stationary wave anomalies. With all forcings present (heavy solid line) the correlation decreases rather uniformly from 0.66 at 1000 hPa to 0.41 at 100 hPa. The forcings responsible for most of the variability also contribute most to the correlation; if the forcing by eddy fluxes is omitted, a substantial fraction of the positive correlation is lost. The importance of the forcing by stationary eddies increases with increasing altitude, evidently matching the behaviour of the stationary wave amplitude. Contrary to the case of the climatological stationary waves, omitting the diabatic heating has now little effect, while omitting the orographic forcing actually improves the correlation at all levels. The method of treating the orographic forcing thus seems too crude to allow for a simulation of the response to anomalous mountain forcing, although it works moderately well for the climatological waves.

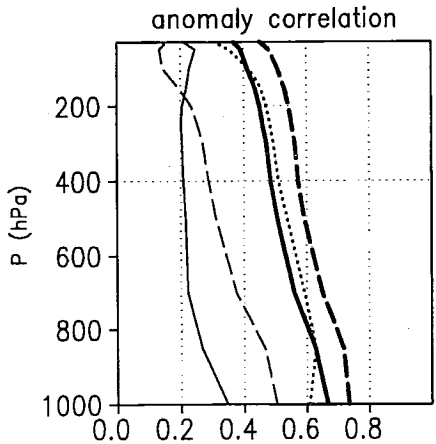

Fig. 8. Vertical profiles of the correlation between observed and computed anomalies to the north of latitude 30°N. The different curves pertain to various combinations of the forcing due to orography (O), diabatic heating (D), transient eddies (T), and stationary eddies (S). Heavy solid line: O+D+T+S, heavy dashed line: D+T+S, dotted line: O+T+S, light solid line: O+D+S, light dashed line: O+D+T.

Examination of the anomaly correlation in individual years (not shown) reveals that in the upper troposphere the relative importance of anomalous forcing by stationary and transient eddies varies from year to year, while in the lower troposphere forcing by the transients always dominates. Omitting the anomalous diabatic heating or orographic forcing does not degrade the simulated anomalies significantly in any of the ten winters.

Further partitioning of the forcing (not shown) indicates that the major reduction in correlation is brought about by omitting the effect of momentum fluxes in the transient eddies, while momentum fluxes in stationary eddies are somewhat less important. Heat fluxes by transient eddies are crucial in the lower troposphere, but no effect of heat fluxes by the stationary eddies can be detected. The importance of

anomalous transient eddy momentum fluxes agrees with the findings of *Branstator* (1992) in that low-frequency anomalies in a perpetual January GCM experiment were maintained by interaction with the time-mean zonal asymmetries and by vorticity forcing of high-frequency transients. Furthermore, anomalous transient eddy momentum fluxes have been found important in forcing extra-tropical anomalies during ENSO episodes (*Kok* and *Opsteegh*, 1985; *Held et al.*, 1989; *Hoerling* and *Ting*, 1994).

5. *Conclusions*

When running the model with various horizontal and vertical resolutions, we found that about 100 grid points between the poles and 10 levels in the vertical produced a simulation in which the rms error due to numerical discretization is at most ~ 10%. In calculating responses to forcing functions inferred from observations, numerical errors of this magnitude are insignificantly small when compared with the errors caused by inaccuracies in the forcing, etc.. In addition, the grid must be dense enough to resolve the distribution of the forcing. We therefore used 16 instead of 10 levels in the vertical for simulating the observed waves.

When the stationary wave forcing is computed from observations, the linear model reproduces the zonal asymmetries in the climatological wintertime middle latitude flow rather successfully. Even the more demanding task of reproducing the observed interannual variability of the zonal asymmetries is performed well enough to hint at the relative importance of the various mechanisms in maintaining the seasonal anomalies.

In all the ten winter seasons examined, anomalies in the stationary waves are maintained principally by anomalous momentum forcing associated with the transient eddies, although in the upper troposphere momentum forcing by the stationary eddies is almost equally important. The direct response to anomalous diabatic heating is not an important contributor to the total variability. Fluctuations in the orographic forcing increased the variability of the total response, but did not improve the correlation between the observed and simulated anomalies. Thus no definite conclusions can be drawn concerning the importance of fluctuations in mountain forcing.

The importance of eddy fluxes seems to indicate that only those anomaly patterns that have the ability to organize these fluxes so as to provide positive feedback survive long enough to contribute to seasonal anomalies. If this idea is correct, similar anomalies might indeed be initiated by quite different external agents which may be hard to identify by a linear analysis.

Our climatological stationary waves simulated with the p coordinate model appear very similar to the waves obtained by VH applying their σ coordinate model. Our results may be somewhat better in the lower troposphere, whereas in the upper troposphere it is difficult to say which of the two simulations is better. An advantage of the present study is that we have used a longer period of observations. On the other

hand, even if our p coordinate model contains the mountain forcing in its complete form ($w_M = ([u] + u^*)(\partial h/\partial x) + v^*(\partial h/\partial y)$), the forcing is applied somewhat arbitrarily at 1000 hPa. Therefore a σ coordinate model may be more applicable for studying the mountain forcing. The contribution of mountain forcing is largest in the upper troposphere and stratosphere. Over mountainous areas in the lower troposphere the σ levels are strongly undulating, and thus deviations from the zonal mean are larger than on isobaric levels. This makes the linear approximation less realistic, and may explain why a p coordinate model works better than a σ coordinate model there.

Perhaps an optimal way of simulating stationary waves with a linear model would be to use σ coordinates for the mountain forcing and p coordinates for other forcings.

Acknowledgments

This investigation is a part of the project "Climate models and scenarios", directed by Eero Holopainen within the Finnish Research Programme on Climate Change (SILMU).

6. *References*

Branstator, G., 1992. The maintenance of low-frequency atmospheric anomalies. *J. Atmos. Sci.*, **49,** 1924-1945.

Fortelius, C., and E. Holopainen, 1990. Comparison of energy source estimates derived from atmospheric circulation data with satellite measurements of net radiation. *J. Climate*, **3**, 646-660.

Fox-Rabinovitz, M.S. and R.S. Lindzen, 1993. Numerical experiments on consistent horizontal and vertical resolution for atmospheric models and observing systems. *Mon. Wea. Rev.*, **121,** 264-271.

Held, I.M., 1983. Stationary and quasi-stationary eddies in the extratropical troposphere: Theory. *Large-scale dynamical processes in the atmosphere*. B. Hoskins and R. Pearce, (Eds), Academic Press, London. 127-168.

Held, I., S. Lyons, and S. Nigam, 1989. Transients and the extratropical response to El Niño. *J. Atmos. Sci.*, **46**, 163-174.

Hoerling, M.P., and M. Ting, 1994. Organization of extratropical transients during El Niño. *J. Climate*, **7**, 745-766.

Hoskins, B.J., H.H. Hsu, I.N. James, M. Masutani, P.D. Sardeshmukh and G.H. White, 1989. Diagnostic of the global atmospheric circulation based on ECMWF analyses 1979-1989. WCRP-27, WMO/TD- No. 326, 217 pp.

Hoskins, B.J. and D.J. Karoly, 1981. The steady linear response of a spherical atmosphere to thermal and orographic forcing. *J. Atmos. Sci.*, **38**, 1179-1196.

Kok, C.J., and J.D. Opsteegh, 1985. Possible causes of anomalies in seasonal mean circulation patterns during the 1982-83 El Niño event. *J. Atmos. Sci.*, **42**, 677-694.

Lindzen, R.S. and M. Fox-Rabinovitz, 1989. Consistent vertical and horizontal resolution. *Mon. Wea. Rev.*, **117**, 2575-2583.

Nigam, S., 1985. On the adequacy of meridional resolution of linear and quasi-linear barotropic models. *J. Atmos. Sci.*, **42**, 2493-2505.

Nigam, S., I.M. Held and S.W. Lyons, 1988. Linear simulation of the stationary eddies in a GCM. Part II: The "mountain" model. *J. Atmos. Sci.*, **45**, 1433-1452.

Ruosteenoja, K., 1988. Need for meridional resolution in linear steady state models using different methods of treating the critical latitude. *J. Atmos. Sci.*, **45**, 3546-3563.

Ruosteenoja, K., 1991. Simulation of the partial reflection by the critical latitude with a linear model. Part II: Stationary wave responses to total forcing. *J. Atmos. Sci.*, **48**, 1529-1534.

Ruosteenoja, K. 1993. An isobaric coordinate multi-layer linear model of stationary waves. Tech. rpt. 8, Dept. of Meteorology, Univ. of Helsinki. 20 pp.

Valdes, P.J. and B.J. Hoskins, 1989. Linear stationary wave simulations of the time-mean climatological flow. *J. Atmos. Sci.*, **46**, 2509-2527.